AD-A048 445 AEROSPACE CORP EL SEGUNDO CALIF IVAN A GETTING LABS F/G 20/4
ESTIMATES OF TURBULENT BOUNDARY LAYER BEHIND A SHOCK WAVE MOVIN--ETC(U)
DEC 77 H MIRELS F04701-77-C-0078
UNCLASSIFIED TR-0078(3781-02)-1 SAMSO-TR-77-166 NL

| OF |
AD
A048445

END
DATE
FILMED
2-78
DDC

REPORT SAMSO-TR-77-166

(12) B.S.

Estimates of Turbulent Boundary Layer Behind a Shock Wave Moving With Uniform Velocity

H. MIRELS
Aerophysics Laboratory
The Ivan A. Getting Laboratories
The Aerospace Corporation
El Segundo, Calif 90245

8 December 1977

Interim Report

Prepared for
DEFENSE NUCLEAR AGENCY
Washington, D.C. 20305

SPACE AND MISSILE SYSTEMS ORGANIZATION
AIR FORCE SYSTEMS COMMAND
Los Angeles Air Force Station
P.O. Box 92960, Worldway Postal Center
Los Angeles, Calif. 90009

This interim report was submitted by The Aerospace Corporation, El Segundo, CA 90245, under Contract No. F04701-77-C-0078 with the Space and Missile Systems Organization, Deputy for Advanced Space Programs, P.O. Box 92960, Worldway Postal Center, Los Angeles, CA 90009. It was reviewed and approved for The Aerospace Corporation by W. R. Warren, Jr., Director, Aerophysics Laboratory. Lieutenant Dara Batki, SAMSO/YCPT, was the project officer for Advanced Space Programs.

This report has been reviewed by the Information Office (OI) and is releasable to the National Technical Information Service (NTIS). At NTIS, it will be available to the general public, including foreign nations.

This technical report has been reviewed and is approved for publication. Publication of this report does not constitute Air Force approval of the report's findings or conclusions. It is published only for the exchange and stimulation of ideas.

Dara Batki

Dara Batki, Lt, USAF
Project Officer

Robert W. Lindemuth

Robert W. Lindemuth, Lt Col, USAF
Chief, Technology Plans Division

FOR THE COMMANDER

Leonard E. Baltzell

LEONARD E. BALTZELL, Col, USAF, Asst.
Deputy for Advanced Space Programs

UNCLASSIFIED

SECURITY CLASSIFICATION OF THIS PAGE (When Data Entered)

REPORT DOCUMENTATION PAGE	READ INSTRUCTIONS BEFORE COMPLETING FORM
1. REPORT NUMBER: SAMSO-TR-77-166	2. GOVT ACCESSION NO.
3. RECIPIENT'S CATALOG NUMBER	
4. TITLE (and Subtitle): ESTIMATES OF TURBULENT BOUNDARY LAYER BEHIND A SHOCK WAVE MOVING WITH UNIFORM VELOCITY.	5. TYPE OF REPORT & PERIOD COVERED: Interim rept.,
6. PERFORMING ORG. REPORT NUMBER: TR-0078(3781-02)-1	
7. AUTHOR(s): Harold Mirels	8. CONTRACT OR GRANT NUMBER(s): F04701-77-C-0078
9. PERFORMING ORGANIZATION NAME AND ADDRESS: The Aerospace Corporation, El Segundo, Calif. 90245	10. PROGRAM ELEMENT, PROJECT, TASK AREA & WORK UNIT NUMBERS
11. CONTROLLING OFFICE NAME AND ADDRESS: Defense Nuclear Agency, Washington, D.C. 20305	12. REPORT DATE: 8 December 1977
	13. NUMBER OF PAGES: 36 (12) 35 p.
14. MONITORING AGENCY NAME & ADDRESS (if different from Controlling Office): Space and Missile Systems Organization, Air Force Systems Command, Los Angeles, Calif. 90009	15. SECURITY CLASS. (of this report): Unclassified
	15a. DECLASSIFICATION/DOWNGRADING SCHEDULE

16. DISTRIBUTION STATEMENT (of this Report)

Approved for public release; distribution unlimited.

17. DISTRIBUTION STATEMENT (of the abstract entered in Block 20, if different from Report)

18. SUPPLEMENTARY NOTES

19. KEY WORDS (Continue on reverse side if necessary and identify by block number)

Boundary Layer
Turbulent Boundary Layer
Shock Waves
Viscous Flow

$1.01 < \alpha = M_s < \alpha = 20$

$3 < \alpha = M_s < = 8$

20. ABSTRACT (Continue on reverse side if necessary and identify by block number)

A theory, previously presented by the author, concerning turbulent boundary-layer development behind a shock moving with uniform speed is briefly reviewed. Numerical results for boundary-layer properties are presented for shock propagation in air at Mach numbers in the range $1.01 \le M_s \le 20$. The heat transfer results are in good agreement with the shock tube wall heat transfer measurements of Hartunian et al., which were made in the range $3 \le M_s \le 8$. Approximate analytical expressions for turbulent boundary-layer properties are deduced.

DD FORM (FACSIMILE) 1473

UNCLASSIFIED 409 944

SECURITY CLASSIFICATION OF THIS PAGE (When Data Entered)

19. KEY WORDS (Continued)

20. ABSTRACT (Continued)

and estimates of the wall temperature variation with distance behind the shock (assumed small) are given. Effects of blowing (wall ablation) are also estimated. The need for experimental data to confirm large Mach number and blowing effects predictions is also noted.

CONTENTS

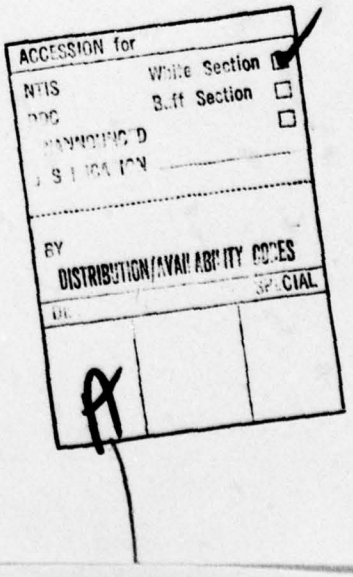

FIGURES

TABLES

I. INTRODUCTION

One basing concept for the MX missile is to have the missile movable within long underground tunnels. In order to estimate the survivability of this system, it is necessary to estimate the rate at which blast-induced air shock waves are attenuated within the tunnel. This requires a knowledge of the turbulent wall boundary layer induced by the shock wave.

A theory for the turbulent boundary-layer development behind a shock wave moving with uniform velocity has been presented[1] and simplifications introduced.[2] Effects of wall blowing (ablation) were not considered. The purpose of the present study is to summarize the previously reported theory (Appendix A), to present numerical results for shock propagation in air (Table 1), to provide approximate analytic expressions (Appendix B), and to provide estimates for effects of blowing (Appendix D). The notation of the previous works[1, 2] is used and is summarized in the Symbols section. The present theory is valid for cases where the increase in wall-surface temperature is small relative to the free-stream recovery temperature. This approximation is examined in Appendix C.

---

[1] H. Mirels, Boundary Layer Behind Shock or Thin Expansion Wave Moving into Stationary Fluid, TN 3712, National Advisory Committee for Aeronautics, (May 1956).

[2] H. Mirels, "Shock Tube Test Time Limitation Due To Turbulent Wall Boundary Layer," AIAA J. 2 (1), 84 (1964).

II. THEORY

In Refs. 1 and 2, the turbulent boundary layer behind a shock moving with uniform speed is considered in shock-fixed coordinates. The flow is steady in this coordinate system and is illustrated in Fig. 1. The wall-surface temperature is assumed to remain at its initial value. Symbols are defined in the Symbols section.

The theoretical development of Refs. 1 and 2 is outlined in Appendix A. Numerical results for the turbulent boundary layer behind a shock propagating into ideal air and real air[3,4] are given in Tables 1a and 1b, respectively. Wall blowing effects are ignored. An initial air temperature $T_1 = 522°R$ is assumed. The results are only weakly dependent on T_1. Measurements of the turbulent heat transfer behind a shock propagating in air have been presented for shock Mach numbers in the range $3 \leq M_s \leq 8$.[5] These results are reproduced in Fig. 2. Comparison with the heat transfer predictions in Table 1b shows good agreement (within a few percent of the mean experimental value at each shock Mach number). This agreement tends to confirm the theory of Refs. 1 and 2 for Mach numbers in the range $M_s \leq 0(10)$ and non-blowing walls.

Turbulent boundary-layer properties of major interest are local boundary thickness, δ; wall shear, $\tau_w = (\mu \partial u/\partial y)_w$; heat transfer to the wall, $-q_w = (k \partial T/\partial y)_w$; and the vertical velocity at the edge of the boundary layer, v_e.

---

[3] C. H. Lewis and E. G. Burgess, III, Charts of Normal Shock Wave Properties in Imperfect Air, AEDC-TDR-64-43, Arnold Engineering Development Center, Air Force Systems Command (March 1964).

[4] C. H. Lewis and E. G. Burgess, III, Charts of Normal Shock Wave Properties in Imperfect Air (Supplement: M_s = 1 to 10), AEDC-TR-65-196, Arnold Engineering Development Center, Air Force Systems Command (September 1965).

[5] R. A. Hartunian, A. L. Russo, and P. V. Marrone, "Boundary Layer Transition and Heat Transfer in Shock Tubes," J. Aerospace Sci. 27, 587 (1960).

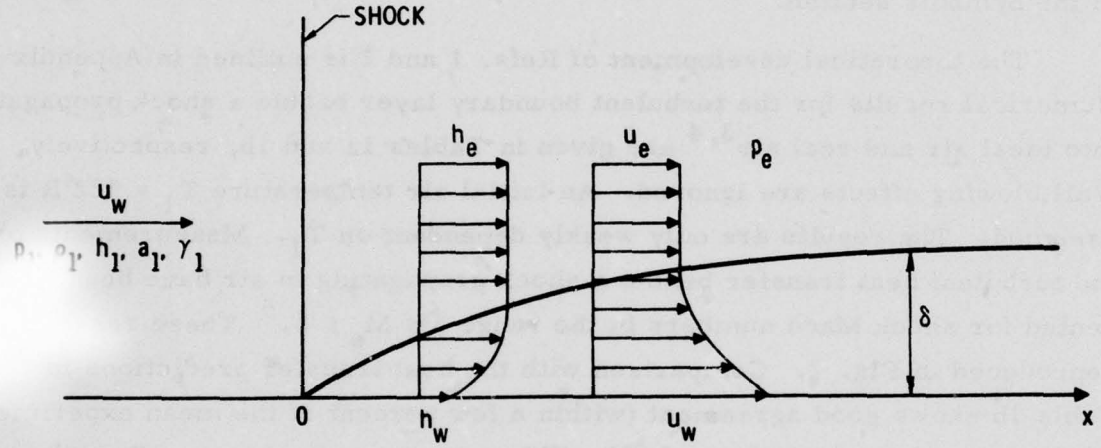

Fig. 1. Boundary Layer Behind Shock in Shock Stationary Coordinates

Table 1a. Turbulent Boundary Layer Behind Shock, Ideal Air ($\gamma = 7/5$)[a]

M_s	W	T_e/T_1	$\frac{\delta^*/\delta}{1-W}$	$\frac{\theta/\delta}{1-W}$	$(p_1x)^{1/5}(\delta)/x$	$(p_1x)^{1/5}(-\delta^*)/x$
1.01	1.0167	1.0066	0.1744	0.1256	0.001110	0.3234E-05
1.10	1.1691	1.0649	0.1698	0.1314	0.004312	0.1238E-03
1.20	1.3416	1.1280	0.1661	0.1378	0.006348	0.3602E-03
1.40	1.6897	1.2547	0.1614	0.1502	0.009060	0.1009E-02
1.60	2.0317	1.3880	0.1588	0.1623	0.010878	0.1782E-02
1.80	2.3592	1.5316	0.1572	0.1740	0.012190	0.2605E-02
2.00	2.6667	1.6875	0.1564	0.1850	0.013174	0.3433E-02
3.00	3.8571	2.6790	0.1557	0.2291	0.015728	0.6996E-02
4.00	4.5714	4.0469	0.1564	0.2570	0.016748	0.9354E-02
5.00	5.0000	5.8000	0.1571	0.2743	0.017263	0.1085E-01
6.00	5.2683	7.9406	0.1576	0.2855	0.017561	0.1181E-01

$(p_1x)^{1/5}(-\theta)/x$	$Re^{1/5}C_H$	$\frac{1}{(p_1d)^{1/4}}\frac{\ell m}{d}$	$\frac{1}{(p_1d)^{5/4}}\overline{Re}_m$	$(p_1x)^{1/5}C_f$	$(p_1x)^{1/5}C_H$	$\frac{(p_1x)^{1/5}}{W-1}\frac{(-v_e)}{u_e}$
0.2330E-05	0.0858	0.1455E+05	0.2605E+08	0.01337	0.008321	0.1549E-03
0.9582E-04	0.0551	0.1320E+04	0.2527E+09	0.00536	0.003337	0.5858E-03
0.2987E-03	0.0489	0.6099E+03	0.4978E+09	0.00410	0.002550	0.8436E-03
0.9387E-03	0.0440	0.2751E+03	0.9865E+09	0.00316	0.001965	0.1170E-02
0.1822E-02	0.0419	0.1725E+03	0.1471E+10	0.00274	0.001705	0.1382E-02
0.2883E-02	0.0408	0.1249E+03	0.1939E+10	0.00250	0.001554	0.1533E-02
0.4062E-02	0.0401	0.9804E+02	0.2379E+10	0.00234	0.001456	0.1648E-02
0.1029E-01	0.0393	0.5096E+02	0.4030E+10	0.00202	0.001256	0.1959E-02
0.1537E-01	0.0396	0.3844E+02	0.4937E+10	0.00193	0.001200	0.2095E-02
0.1894E-01	0.0399	0.3318E+02	0.5436E+10	0.00189	0.001179	0.2169E-02
0.2140E-01	0.0402	0.3044E+02	0.5728E+10	0.00188	0.001170	0.2214E-02

[a]Data are based on Appendix A.
$Pr = 0.72$, $h_w = h_1$, $T_1 = 522^\circ R$;
p_1 is in atmospheres, x is in feet.

Table 1b. Turbulent Boundary Layer Behind Shock, Real Air (Refs. 3 and 4)[a]

M_s	W	T_e/T_1	$\frac{\delta^*/\delta}{1-W}$	$\frac{\theta/\delta}{1-W}$	$(p_1x)^{1/5}(\delta)/x$	$(p_1x)^{1/5}(-\delta^*)/x$
2.00	2.6700	1.6900	0.1563	0.1851	0.013187	0.3442E-02
3.00	3.9500	2.6500	0.1549	0.2319	0.015849	0.7241E-02
4.00	4.8500	3.8500	0.1546	0.2655	0.016938	0.1008E-01
5.00	5.5500	5.3000	0.1541	0.2914	0.017534	0.1229E-01
6.00	6.1300	6.9500	0.1535	0.3124	0.017891	0.1409E-01
7.00	6.6500	8.7000	0.1528	0.3308	0.018109	0.1563E-01
8.00	7.2000	10.7000	0.1518	0.3496	0.018302	0.1723E-01
10.00	8.3000	14.3000	0.1501	0.3865	0.018435	0.2020E-01
12.00	9.0500	18.1000	0.1492	0.4117	0.018405	0.2210E-01
14.00	9.4000	22.4000	0.1489	0.4236	0.018323	0.2291E-01
16.00	9.9000	26.3000	0.1483	0.4402	0.018219	0.2405E-01
18.00	10.5500	29.7000	0.1476	0.4614	0.018095	0.2551E-01
20.00	11.1500	32.5000	0.1470	0.4810	0.017935	0.2676E-01

$(p_1x)^{1/5}(-\theta)/x$	$Re^{1/5}C_H$	$\frac{1}{(p_1d)^{1/4}}\frac{t_m}{d}$	$\frac{1}{(p_1d)^{5/4}}\bar{R}e_m$	$(p_1x)^{1/5}C_f$	$(p_1x)^{1/5}C_H$	$\frac{(p_1x)^{1/5}}{W-1}\frac{(-v_e)}{u_e}$
0.4076E-02	0.0401	0.9782E+02	0.2380E+10	0.00234	0.001456	0.1649E-02
0.1084E-01	0.0391	0.4941E+02	0.4195E+10	0.00199	0.001241	0.1964E-02
0.1732E-01	0.0392	0.3590E+02	0.5518E+10	0.00187	0.001163	0.2095E-02
0.2325E-01	0.0392	0.2952E+02	0.6586E+10	0.00180	0.001118	0.2162E-02
0.2867E-01	0.0392	0.2578E+02	0.7539E+10	0.00174	0.001085	0.2197E-02
0.3384E-01	0.0392	0.2323E+02	0.8504E+10	0.00170	0.001056	0.2213E-02
0.3968E-01	0.0390	0.2106E+02	0.9489E+10	0.00165	0.001028	0.2223E-02
0.5202E-01	0.0387	0.1793E+02	0.1201E+11	0.00156	0.000972	0.2214E-02
0.6099E-01	0.0385	0.1636E+02	0.1413E+11	0.00151	0.000937	0.2196E-02
0.6520E-01	0.0384	0.1577E+02	0.1549E+11	0.00148	0.000920	0.2182E-02
0.7137E-01	0.0383	0.1501E+02	0.1742E+11	0.00144	0.000897	0.2162E-02
0.7974E-01	0.0381	0.1413E+02	0.1995E+11	0.00140	0.000871	0.2137E-02
0.8756E-01	0.0379	0.1345E+02	0.2276E+11	0.00136	0.000846	0.2109E-02

[a]Data are based on Appendix A.
Pr = 0.72, $h_w = h_1$, T = 522°R;
P_1 is in atmospheres, x is in feet.

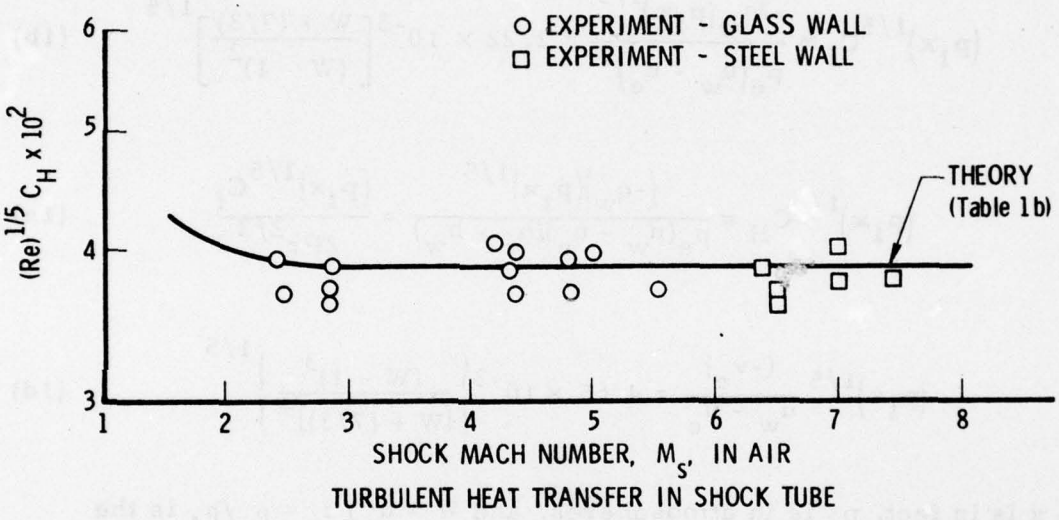

Fig. 2. Comparison of Present Theory With Experimental Data of Ref. 5

Approximate analytic expressions for these quantities are given in Appendix B. These are, for $W > 1.02$ and $T_1 = 522°R$

$$(p_1 x)^{1/5} \delta/x = 0.0370 \left\{ \frac{(W-1)^3}{[W + (7/3)]^4} \right\}^{1/5} \tag{1a}$$

$$(p_1 x)^{1/5} C_f \equiv \frac{-2\tau_w (p_1 x)^{1/5}}{\rho_e (u_w - u_e)^2} = 2.22 \times 10^{-3} \left[\frac{W + (7/3)}{(W-1)^2} \right]^{1/5} \tag{1b}$$

$$(p_1 x)^{1/5} C_H \equiv \frac{(-q_w)(p_1 x)^{1/5}}{\rho_e (u_w - u_e)(h_r - h_w)} = \frac{(p_1 x)^{1/5} C_f}{2 Pr^{2/3}} \tag{1c}$$

$$(p_1 x)^{1/5} \frac{(-v_e)}{u_w - u_e} = 4.65 \times 10^{-3} \left\{ \frac{(W-1)^3}{[W + (7/3)]^4} \right\}^{1/5} \tag{1d}$$

where x is in feet, p_1 is in atmospheres, and $W = u_w/u_e = \rho_e/\rho_1$ is the velocity (density) ratio across the shock. Other symbols are defined in the Symbols section. Equations (1a) through (1d) agree with the numerical results in Table 1 to within about 10%. The quantities C_f, C_H, and v_e are normalized by the use of $u_w - u_e$, which is the free-stream velocity in laboratory (wall stationary) coordinates. It is seen that v_e is negative, i.e., the vertical velocity at the edge of the boundary layer is directed toward the wall. This is the result of the aspirating effect of the wall in shock-fixed coordinates (Fig. 1).

The theory of Refs. 1 and 2 assumes that the departure of the wall-surface temperature, T_w, from its initial value, T_1, is negligible. In

Appendix C, the variation of wall-surface temperature with distance behind the shock is shown to equal (for strong shocks)

$$\frac{1}{p_1^{0.8} x^{0.3}} \left(\frac{T_w}{T_1} - 1 \right) = E M_s^{5/2} W^{4/5} \left[1 + 0\left(\frac{1}{W}\right) \right] \tag{2a}$$

where E is a function of wall material; typical values (from Carslaw and Yaeger[6]) are given in Table 2. The present theory is valid when the change in wall-surface temperature is small relative to the recovery temperature T_r. For strong shocks, the latter ratio is found from

$$\frac{1}{p_1^{0.8} x^{0.3}} \frac{T_w - T_1}{T_r} = \frac{E}{0.38} M_s^{1/2} W^{4/5} \left[1 + 0\left(\frac{1}{W}\right) \right] \tag{2b}$$

The above equations neglect ablation, which tends to limit the wall-surface temperature increase and therefore to extend the region of validity of the present results. However, the effects of blowing on the boundary-layer properties need to be considered. These effects are treated in Appendix D.

The effect of blowing on boundary-layer properties at a fixed x location can be expressed by

$$\frac{C_H}{(C_H)_0} = \frac{C_f}{(C_f)_0} = \frac{\ell n(1 + B')}{B'} \tag{3a}$$

$$\frac{\delta}{\delta_0} = \frac{\delta^*}{\delta_0^*} = \frac{\theta}{\theta_0} = \frac{(1 + B')\ell n(1 + B')}{B'} \tag{3b}$$

[6] H. S. Carslaw and J. C. Yaeger, Conduction of Heat in Solids, Oxford University Press (1959), pp. 76, 496.

Table 2. Approximate Thermal Properties of the Wall[a]

Type	Material	$(\rho\overline{C}k)_b^{1/2}$, $\frac{cal}{cm^2\ °K\ (sec)^{1/2}}$	E,[b] $\left(\frac{1}{atm}\right)^{0.8}\left(\frac{1}{ft}\right)^{0.3}$
Metal	Aluminum	5.17×10^{-1}	3.92×10^{-4}
	Mild steel (0.1% c)	3.19×10^{-1}	6.34×10^{-4}
	Cast iron	3.48×10^{-1}	5.82×10^{-4}
Nonmetal	Glass (crown)	3.67×10^{-2}	5.52×10^{-3}
	Concrete (1:2:4)	3.41×10^{-2}	5.93×10^{-3}
Gas	Air	1.34×10^{-4}	1.51×10^{0}

[a] From Ref. 6

[b] $E = 2.024 \times 10^{-4}/(\rho\overline{C}k)_b^{1/2}$

where subscript zero denotes the local nonblowing value [given by Eqs. (1a) through (1d)] and

$$B' \equiv \frac{(\rho v)_w}{\rho_e |u_w - u_e| C_H} = \frac{hr}{\Delta H} \tag{3c}$$

Here ΔH is the difference between the enthalpy of the unheated wall material and the wall material at the gas/wall interface (i.e., the effective heat of ablation of the wall material). The effect of blowing on v_e is given in Eq. (D-10).

The present results are applicable for a shock propagating in a tube of diameter d provided that $2\delta/d \ll 1$ (i.e., the boundary layer is thin relative

to the tube radius). The present results can be taken as approximately correct for values of $2\delta/d$ up to about 1. Boundary-layer closure (i.e., $2\delta/d = 1$) occurs at

$$\left(\frac{x}{d}\right)_c = \left(p_1 d\right)^{1/4} / \left[2\left(p_1 x\right)^{1/5} (\delta/x)\right]^{5/4} \tag{4a}$$

$$= 65\left(p_1 d\right)^{1/4} (1 \pm 0.05) \quad M_s \geq 4 \tag{4b}$$

Equation (4b) applies for nonblowing cases. Blowing causes boundary-layer closure to occur at smaller values of x. The closure stations for the blowing and nonblowing cases are related by [e.g., Eq. (D-11)]

$$\frac{x_c}{(x_c)_0} = \left[\frac{B'}{(1 + B')\ell n(1 + B')}\right]^{5/4} \tag{4c}$$

The flow downstream of x_c is fully developed. The shear and heat transfer in this region are on the order of the shear and heat transfer at x_c.

The present results can be used to estimate shock attenuation for cases where $2\delta/d \ll 1$. The effect of the boundary layer on the inviscid flow external to the boundary layer is found from a distribution of volumetric mass sources defined by[7]

$$\dot{M} \equiv \frac{4}{d} \rho_e v_e \qquad \frac{\text{mass addition}}{\text{volume-time}} \tag{5}$$

where v_e is evaluated by use of Eqs. (1d) or (D-8). A combination of volumetric momentum and energy sources is needed when the flow is fully developed and the wall is nonblowing. Mass sources must be included in the

[7] H. Mirels and J. F. Mullen, "Small Perturbation Theory For Shock Tube Attenuation and Non Uniformity," Phys. Fluids 7 (8), 1208 (1964).

fully developed flow regime with wall blowing. Further discussion of wall effects on shock propagation is beyond the scope of the present study.

III. CONCLUDING REMARKS

The present results are intended to facilitate estimates of the turbulent boundary layer behind shocks moving in air. The results are expected to be fairly accurate for nonblowing walls and for $M_s \leq 0(10)$ (e.g., Fig. 2). Further study is required in order to validate the results for $M_s > 10$ and a nonblowing wall. Effects of blowing may be considered uncertain for all M_s. Further comparisons with experiment and comparisons with numerical results from more accurate turbulent boundary-layer codes are desirable for $M_s > 10$ and for wall blowing.

APPENDIX A

BOUNDARY-LAYER CHARACTERISTICS

Characte[illegible]emi-infinite, zero-pressure-gradient, steady-state tur[illegible]dary layer are summarized herein for the case of a moving wall. [illegible]ions for the boundary layer behind a shock, moving with unifcrm speed, are then noted. These results are based on the theoretical development in Refs. 1 and 2.

1. GENERAL MOVING WALL

Consider a zero-pressure-gradient turbulent boundary layer with a moving wall in a coordinate system in which mean properties are steady state (e.g., Fig. 1). The wall velocity is denoted u_w, and the free-stream velocity is denoted u_e. Following the development in Ref. 1, the boundary-layer thickness, δ^*, and momentum thickness, θ, are related by

$$\frac{\theta/\delta}{1-W} = 7\frac{h_e}{h_w}\int_0^1 \frac{\zeta^6[W - (2W-1)\zeta + (W-1)\zeta^2]\,d\zeta}{1 + b\zeta - c\zeta^2} \qquad \text{(A-1a)}$$

$$\frac{\delta^*/\delta}{1-W} = \frac{1}{1-W}\left\{1 - 7\frac{h_e}{h_w}\int_0^1 \frac{\zeta^6[W - (W-1)\zeta]d\zeta}{1 + b\zeta - c\zeta^2}\right\} \qquad \text{(A-1b)}$$

where

$$b = \frac{h_r}{h_w} - 1 \qquad \text{(A-2a)}$$

$$c = \left(\frac{h_r}{h_e} - 1\right)\frac{h_e}{h_w} \qquad \text{(A-2b)}$$

$$\frac{h_r}{h_e} = 1 + \frac{r(o)}{2} \frac{(W - 1)^2 u_e^2}{h_e} \qquad \text{(A-2c)}$$

Here $W = u_w/u_e$, and $r(o) = Pr^{1/3}$ is the recovery factor. The boundary-layer thickness was found to equal

$$\frac{\delta}{x} = 0.0574 \left[\left(\frac{1-W}{\theta/\delta} \right)^4 |1 - W|^3 \left(\frac{\mu_m}{\mu_e} \right) \left(\frac{\rho_m}{\rho_e} \right)^3 \left(\frac{\nu_e}{u_e x} \right) \right]^{1/5} \qquad \text{(A-3)}$$

where subscript m denotes a mean value defined by

$$\frac{h_m}{h_e} = 0.5 \left(\frac{h_w}{h_e} + 1 \right) + 0.22 \left(\frac{h_r}{h_e} - 1 \right) \qquad \text{(A-4)}$$

Corresponding values of δ^* and θ are found from Eqs. (A-1a) and (A-1b). Noting that $d\delta/dx = (4/5)(\delta/x)$, we find the shear and heat transfer from

$$\frac{\tau_w}{\rho_e u_e^2} = \frac{Pr^{2/3}(W - 1)}{\rho_e u_e (h_r - h_w)} \quad q_w = \frac{d\theta}{dx} = \frac{4}{5} \left(\frac{\theta}{\delta} \right) \frac{\delta}{x} \qquad \text{(A-5)}$$

where $\tau_w \equiv (\mu \partial u/\partial y)_w$ and $-q_w \equiv (k \partial T/\partial y)_w$. The vertical velocity at the edge of the boundary layer, v_e, is obtained from

$$\frac{v_e}{u_e} = \frac{d\delta^*}{dx} = \frac{4}{5} \left(\frac{\delta^*}{\delta} \right) \frac{\delta}{x} \qquad \text{(A-6)}$$

Local shear and heat transfer coefficients may be expressed in the form

$$C_f \equiv \frac{-2\tau_w}{\rho_e (u_w - u_e)\,|u_w - u_e|} = \frac{1.6}{|W - 1|}\left(\frac{\theta/\delta}{1 - W}\right)\frac{\delta}{x} \qquad \text{(A-7a)}$$

$$C_H \equiv \frac{-q_w}{\rho_e\,|u_w - u_e|\,(h_r - h_w)} = \frac{0.8}{\rho_r^{2/3}\,|W - 1|}\left(\frac{\theta/\delta}{1 - W}\right)\frac{\delta}{x} \qquad \text{(A-7b)}$$

The latter are positive quantities and are referenced to "wall fixed" quantities. (Note that $|u_w - u_e|$ is the velocity of the free stream relative to the wall.) It follows from Eqs. (A-5) and (A-7) that $C_f/2 = Pr^{2/3}\, C_H$. With the introduction of a Reynolds number, $R_e \equiv |u_w - u_e|\, x/\nu_e$, it follows that

$$Re^{1/5}\, C_H = \frac{0.0459}{Pr^{2/3}}\left[\frac{\theta/\delta}{1 - W}\,\frac{(\mu_m/\mu_e)\,(\rho_m/\rho_e)^3}{|W - 1|}\right]^{1/5} \qquad \text{(A-8)}$$

In the limit $W = 0$, the above equations define the boundary layer over a semi-infinite flat plate. The case $W > 1$ corresponds to flow behind a shock wave moving with uniform velocity and is considered in the next section.

In Ref. 1, Eqs. (A-1) through (A-8) were derived on the basis of an ideal gas, namely, $h \sim T \sim \rho^{-1}$ at constant pressure. The present form, following Ref. 2, attempts to reduce the sensitivity to this assumption to some extent.

2. BOUNDARY LAYER BEHIND SHOCK

We consider a shock moving with uniform velocity, $u_s = u_w$, into air. Undisturbed air conditions are denoted by subscript 1 (Fig. 1). We assume $\gamma_1 = 7/5$, $Pr = 0.72$, $r(o) = 0.90$, $T_w = T_1 = 522°R$,* and $h_w = h_1$. The latter assumption is discussed in Appendix C. Corresponding values of M_s, $W = u_w/u_e = \rho_e/\rho_w$, and T_e/T_1 are found from ideal or real gas (Refs. 3 and 4)

*The solution is relatively insensitive to the assumption $T_1 = 522°R$. For $\mu \sim T^\omega$, it can be shown $\delta \sim T_1^{0.2\omega + 0.1}$.

shock relations. Noting $0.7 \leq (h_m/h_e) \leq 1.0$, we further assume that $T_m/T_1 = (h_m/h_e)(T_e/T_1)$ and $\rho_m/\rho_e = h_e/h_m$, where h_m/h_e is found from Eq. (A-4) and

$$\frac{h_e}{h_1} = 1 + 0.2\, M_s^2 \left(1 - \frac{1}{W^2}\right) \tag{A-9a}$$

$$\frac{h_r}{h_e} = 1 + \frac{0.18\, M_s^2}{h_e/h_1} \left(\frac{W - 1}{W}\right)^2 \tag{A-9b}$$

For air at $T_1 = 522°\,R$

$$\left(\frac{\rho a}{p\mu}\right)_1 = 6.93 \times 10^6 \quad (\text{atm-ft})^{-1} \tag{A-10}$$

where p_1 is in atmospheres. The Sutherland relation for the viscosity of air is

$$\frac{\mu}{\mu_1} = \left(\frac{T}{T_1}\right)^{3/2} \frac{T_1 + 198.6}{T + 198.6} \tag{A-11}$$

where T is in degrees Rankine. Boundary-layer paramenters can then be found from

$$(p_1 x)^{1/5} \frac{\delta}{x} = 2.46 \times 10^{-3} \left[\left(\frac{1 - W}{\theta/\delta}\right)^4 (W - 1)^3 \left(\frac{h_e}{h_m}\right)^3 \frac{\mu_m/\mu_1}{M_s}\right]^{1/5} \tag{A-12a}$$

$$(p_1 x)^{1/5} \left(\frac{-\delta^*}{x}\right) = \left[(p_1 x)^{1/5} \frac{\delta}{x}\right] \left(\frac{\delta^*/\delta}{1 - W}\right) (W - 1) \qquad \text{(A-12b)}$$

$$(p_1 x)^{1/5} \left(\frac{-\theta}{x}\right) = \left[(p_1 x)^{1/5} \frac{\delta}{x}\right] \left(\frac{\theta/\delta}{1 - W}\right) (W - 1) \qquad \text{(A-12c)}$$

where the dimensions of $p_1 x$ are in atmosphere-feet. The quantities τ_w, q_w, and v_e are found from Eqs. (A-5) and (A-6). Also

$$Re^{1/5} C_H = 0.0572 \left[\frac{\theta/\delta}{1 - W} \left(\frac{h_e}{h_m}\right)^3 \frac{\mu_m/\mu_e}{(W - 1)}\right]^{1/5} \qquad \text{(A-12d)}$$

In a shock tube of diameter d, operating at its maximum test time, the separation between the contact surface and the shock is denoted by ℓ_m and is found from (Ref. 2)

$$\frac{1}{(p_1 d)^{1/4}} \frac{\ell_m}{d} = \frac{0.1768\ W\ (W - 1)}{W^2 + 1.25\ W - 0.80} \left[(p_1 x)^{1/5} \left(\frac{-\delta^*}{x}\right)\right]^{-5/4} \qquad \text{(A-13)}$$

An equivalent flat plate Reynolds number, based on the distance that a free-stream particle has moved relative to the wall, is** $\bar{R}e = u_e (W - 1)^2 x / \nu_e$. The value of $\bar{R}e$ at the contact surface is

$$\frac{1}{(p_1 d)^{5/4}} \bar{R}e_m = 6.93 \times 10^6 M_s \frac{\mu_1}{\mu_e} (W - 1)^2 \left[\frac{\ell_m}{d} \frac{1}{(p_1 d)^{1/4}}\right] \qquad \text{(A-14)}$$

Turbulent theory is applicable, provided $\bar{R}e_m$ is of order 10^7 or greater.

**$\bar{R}e$ is not to be confused with Re.

Equations (A-12) through (A-14) have been evaluated numerically, and the results are presented in Table 1. Similar results were presented graphically in Ref. 2. In Fig. 2, the results for $Re^{1/5}C_H$ are compared with the experiments of Ref. 5, and good agreement is observed.

APPENDIX B

APPROXIMATE ANALYTIC FORMULATION

Approximate analytic expressions for boundary-layer properties can be obtained by use of the approximate expressions for Eq. (B-1) presented in Ref. 2. For ideal gases, the latter are

$$\frac{\theta/\delta}{1-W} \doteq \frac{3W+7}{80} \qquad \gamma = 7/5 \qquad \text{(B-1a)}$$

$$\doteq \frac{W+2}{24} \qquad \gamma = 5/3 \qquad \text{(B-1b)}$$

$$\frac{\delta^*/\delta}{1-W} \doteq 0.157 \qquad \gamma = 7/5,\ W \geq 2 \qquad \text{(B-1c)}$$

$$\doteq 0.176 \qquad \gamma = 5/3,\ W \geq 2 \qquad \text{(B-1d)}$$

Equations (B-1a) through (B-1d) are correct to within 8% for strong shocks in air with $W \leq 15$.

Consider the case of a strong shock moving into air. Neglecting terms of order $1/M_s^2$, $1/W$, and h_w/h_e compared with 1, we find $h_e/h_1 = 0.2\ M_s^2$, $h_r/h_e = 1.9$, and $h_m/h_e = 0.700$. Also, for $T_1 = 522°R$ and $198.6/T_m \ll 1$, the Sutherland relation becomes $\mu_m/\mu_1 = 1.380\ (T_m/T_1)^{1/2}$. Then, if it is assumed that $T_m/T_1 = h_m/h_1 = 0.14\ M_s^2$, the viscosity law becomes $\mu_m/\mu_1 = 0.524\ M_s$. Substitution of the relations

$$\left.\begin{aligned} \mu_m/\mu_1 &= 0.524\ M_s \\ h_m/h_e &= 0.700 \end{aligned}\right\} \qquad \text{(B-2)}$$

and Eq. (B-1a) into Eq. (A-12a) yields

$$(p_1 x)^{1/5} \frac{\delta}{x} = 0.0370 \left\{ \left[\frac{(W-1)^3}{[W + (7/3)]^4} \right] \right\}^{1/5} \qquad \text{(B-3)}$$

Equation (B-3) is in remarkably good agreement with all the numerical results in Table 1, including W near 1, since δ/x is relatively insensitive to the approximations used to obtain Eq. (B-2). Equation (B-3) agrees with the real gas results in Table 1b to within 5% and with the ideal gas results in Table 1a (including the range $1.02 \leq W \leq 6$) to with 10%. Hence, all boundary-layer properties of interest can be deduced from Eqs. (B-1) and (B-3) with an accuracy of about 10%. In particular, the shear, heat transfer, and mass loss to the boundary layer may be expressed [from Eqs. (A-7) (B-1), and (B-3)]

$$(p_1 x)^{1/5} C_f = 2\, Pr^{2/3} (p_1 x)^{1/5} C_H$$

$$= 2.22 \times 10^{-3} \left[\frac{W + (7/3)}{(W-1)^2} \right]^{1/5} \qquad \text{(B-4a)}$$

$$\frac{(p_1 x)^{1/5}}{W-1} \frac{(-v_e)}{u_e} = 4.65 \times 10^{-3} \left[\left\{ \frac{(W-1)^3}{[W + (7/3)]^4} \right\} \right]^{1/5} \qquad \text{(B-4b)}$$

These equations agree with the numerical results in Table 1 to within about 10%.

APPENDIX C

WALL-SURFACE TEMPERATURE

In Appendix A, it was assumed that the wall-surface temperature, T_w, remains constant at its original value, T_1. The validity of this assumption is examined herein for the case of a turbulent boundary layer behind a moving shock.

The transformation $t = x/u_w$ relates the variation with time at a fixed point on the wall (laboratory coordinates) with the variation with distance behind the shock, x, in shock-fixed coordinates. Hence, in laboratory coordinates, the heat transfer to the wall, as a function of time after shock passage, has the form $-q_w \sim t^{-1/5}$. The departure of wall-surface temperature, T_w, from its initial value, T_1, can be found from (Ref. 6)

$$T_w - T_1 = \frac{(-q_w)t^{1/5}}{\sqrt{\pi}\sqrt{(\rho\bar{C}k)_b}} \int_o^t \frac{d\tau}{(t-\tau)^{1/5}\,\tau^{1/2}} \qquad \text{(C-1)}$$

where $(\rho\bar{C}k)_b$ is the product of density, specific heat, and thermal conductivity of the wall ("body") material. Dependence of the latter properties on temperature is neglected. Introduction of the beta function $\beta(0.5, 0.8) = 1.297\sqrt{\pi}$ permits Eq. (C-1) to be written in the form

$$T_w - T_1 = \frac{1.297\,(-q_w)t^{1/2}}{\sqrt{(\rho\bar{C}k)_b}} \qquad \text{(C-2)}$$

Expressing $(-q_w)$ in terms of C_H then yields

$$\frac{1}{p_1\sqrt{x}}\left(\frac{T_w}{T_1} - 1\right) = \frac{1.297}{\sqrt{(\rho\bar{C}k)_b}}\left(\frac{\rho h a^{1/2}}{pT}\right)_1 \sqrt{M_s}\left[(W - 1)\frac{h_r}{h_1}\left(1 - \frac{h_w}{h_r}\right)C_H\right] \quad (C-3)$$

Thermal properties of typical wall materials are given in Table 2 in cgs-cal-°K units. In similar units

$$\left(\frac{\rho h a^{1/2}}{pT}\right)_1 = 0.05383 \frac{cal}{cm^{5/2}\ sec^{1/2}\ atm°K} \quad (C-4)$$

for air at a temperature of 290° K (522° R). Substitution of these quantities into Eq. (C-3) provides the variation of wall temperature, T_w, as a function of distance x in cm. Since $C_H \sim (p_1 x)^{-1/5}$, it follows that $(T_w - T_1) \sim p_1^{0.8} x^{0.3}$.

In the limit of a strong shock in air, Eq. (C-3) can be expressed in the form

$$\frac{1}{p_1^{0.8} x^{0.3}}\left(\frac{T_w}{T_1} - 1\right) = E\, M_s^{5/2}\, W^{4/5}\left[1 + 0\left(\frac{1}{W}\right)\right] \quad (C-5)$$

where p_1 and x are in atmospheres and feet, respectively, and $E = 2.024 \times 10^{-4}/(\rho\bar{C}k)_b^{1/2}$. Equation (C-5) employs Eq. (B-4a) and assumes $h_r/h_1 = 0.38\, M_s^2$, $h_w/h_r \ll 1$. Values of E are tabulated in Table 2 for various wall materials. The quantity E is of order 5×10^{-4} for metal walls and of order 5×10^{-3} for nonmetal walls. The boundary-layer solution in Appendix A assumed $T_w = T_1$. The increase in wall-surface temperature with x has a small effect on this boundary-layer solution if $T_w - T_1$ is small relative to the recovery (adiabatic) temperature, T_r. Assuming $T_r/T_1 = 0.38\, M_s^2$, we can express Eq. (C-5) by

$$\frac{1}{p_1^{0.8}\, x^{0.3}} \frac{T_w - T_1}{T_r} = \frac{E}{0.38} M_s^{1/2}\, W^{4/5} \left[1 + 0\left(\frac{1}{W}\right)\right] \qquad \text{(C-6)}$$

In general, $(T_w - T_1)/T_r$ is small; thus, the variation of wall-surface temperature need not be considered in the boundary-layer equations. However, $(T_w - T_1)/T_1$ may become sufficiently large that melting, or ablation, occurs for very strong shocks. In the latter case, Eqs. (C-5) and (C-6) are inapplicable. For example, if $M_s = 10$, $W = 8.3$, the right-hand sides of Eqs. (C-5) and (C-6) become 1.0 and 0.03, respectively, for metallic walls. The present solution is then consistent and applicable for p_1 of order 1 atm and x of order 1 ft. However, for nonmetallic walls, under the same flow conditions, the right-hand sides of Eqs. (C-5) and C-6) are approximately 10 and 0.3, respectively, and some ablation may occur at distances on the order of 1 ft or greater behind the shock. Ablation will tend to limit the wall-surface temperature rise and, thus, make the present assumption $h_w/h_r \ll 1$ valid, but the effect of wall blowing must be taken into account. This is done in Appendix D.

APPENDIX D

WALL BLOWING EFFECTS

The effect of blowing on wall shear and heat transfer is not well established for turbulent boundary layers. No experimental data are available for the case of a turbulent boundary layer behind a moving shock. Nevertheless, an estimate of this effect, based on results for semi-infinite flat plates, is presented herein. The blown gas is assumed to be air-like.

Based on the flat-plate analogy,[8,9] the ratio of blowing to nonblowing (subscript zero) shear and heat transfer may be expressed by

$$\frac{C_H}{(C_H)_0} = \frac{C_f}{(C_f)_0} = \frac{B}{e^B - 1} \tag{D-1a}$$

$$= \frac{\ln (1 + B')}{B'} \tag{D-1b}$$

where

$$B \equiv \frac{(\rho v)_w}{\rho_e |u_w - u_e| (C_H)_0} \tag{D-2a}$$

[8] W. H. Dorrance, Viscous Hypersonic Flow, McGraw-Hill (1962), pp. 59, 206-220.

[9] W. M. Kays and R. J. Moffat, "The Behavior of Transpired Turbulent Boundary Layers," in Studies in Convection, ed. B. E. Launder, Academic Press, New York (1975), p. 251.

$$B' \equiv \frac{(\rho v)_w}{\rho_e |u_w - u_e| C_H} \qquad \text{(D-2b)}$$

Note that

$$B = \ln (1 + B')$$

If we assume that all the thermal conduction from the air to the wall results in ablation of wall material (i.e., thermal conduction within the wall is neglected), it follows that

$$-q_w = (\rho v)_w \Delta H \qquad \text{(D-3)}$$

where ΔH is the heat of ablation of the wall material. (More generally, ΔH is the difference in enthalpy between the unheated wall material and the wall material at the air/wall interface.) Equation (D-2b) can then be expressed as

$$B' = \frac{h_r - h_w}{\Delta H} = \frac{h_r}{\Delta H} \qquad \text{(D-4)}$$

and the effect of blowing on wall shear and heat transfer can be readily deduced from Eq. (D-1b). The value of B' can be readily estimated. For air at an initial temperature of 522° R, $h_1 = 69.4$ cal/gr. Thus, for strong shocks, $h_r = 0.38\, M_s^2\, h_1 = 26.4\, M_s^2$ cal/gr. For a vaporizing (T = 3100° K) steel wall, $\Delta H = 2100$ cal/gr and $B' = 1.25$, 5.00, and 125 for $M_s = 10$, 20, and 100, respectively.

The variation of boundary-layer momentum thickness with distance is of interest. The momentum integral equation

$$\rho_e u_e^2 \frac{d\theta}{dx} = \tau_w + (\rho v)_w (u_e - u_w) \qquad \text{(D-5a)}$$

can be expressed in the form

$$\frac{-1}{(W-1)^2} \frac{d\theta}{dx} = \frac{C_f}{2} + \frac{(\rho v)_w}{\rho_e u_e (W-1)} \qquad \text{(D-5b)}$$

Taking the Reynolds analogy to be $C_f = 2C_H$, substituting from Eq. (D-1b), and integrating, we obtain, at a fixed x

$$\frac{\theta}{\theta_0} = \frac{(1+B')\ln(1+B')}{B'} \qquad \text{(D-6)}$$

from which momentum thickness can be obtained. The vertical velocity at the edge of the boundary layer is also of interest. The latter can be expressed by

$$\frac{v_e}{u_e} = \frac{d\delta^*}{dx} + \frac{(\rho v)_w}{\rho_e u_e} \qquad \text{(D-7)}$$

Assuming δ^*/δ_0^* is independent of x and recalling $d\delta_0^*/dx = (4/5)(\delta_0^*/x)$, we can express Eq. (D-7) as

$$\frac{v_e}{(v_e)_0} = \frac{\delta^*}{\delta_0^*}\left[1 - \frac{\ln(1+B')}{\frac{4}{5}\frac{\delta^*}{\delta_0^*}\left(\frac{\delta_0^*/\delta_0}{1-W}\right)} \cdot \frac{(p_1 x)^{1/5}(C_H)_0}{(p_1 x)^{1/5}\frac{\delta_0}{x}}\right] \qquad \text{(D-8)}$$

The ratio δ^*/δ_0^* is needed. If it is assumed that the form factors δ^*/δ and θ/δ are unchanged by blowing (which is highly unlikely), then, at a fixed x

$$\frac{\delta^*}{\delta_0^*} = \frac{\delta}{\delta_0} = \frac{\theta}{\theta_0} = \frac{(1 + B') \ln (1 + B')}{B'} \qquad \text{(D-9)}$$

The validity of Eq. (D-9) requires further study. In the absence of better estimates, Eq. (D-9) can be used to evaluate δ^*/δ_0^* in Eq. (D-8). Substitution of Eqs. (B-1c), (B-3), and (B-4a) into Eq. (D-8) then yields, for air (Pr = 0.9)

$$\frac{v_e}{(v_e)_0} = \frac{(1 + B') \ln (1 + B')}{B'} \left[1 - \frac{0.256B'}{1 + B'} \left(\frac{W + (7/3)}{W - 1}\right)\right] \qquad \text{(D-10a)}$$

$$= \frac{(1 + 0.744B') \ln (1 + B')}{B'} \quad \text{for } W \gg 1 \qquad \text{(D-10b)}$$

When $W \gg 1$, wall blowing increases $v_e/(v_e)_0$.

The rate of growth of the boundary-layer thickness, δ, for blowing and nonblowing cases can also be compared. Let x and x_0 denote the corresponding axial stations for blowing and nonblowing cases, respectively, where the boundary-layer thickness has the same value. Since $\delta \sim x^{4/5}$, Eq. (D-9) indicates that for fixed δ

$$\frac{x}{x_0} = \left[\frac{B'}{(1 + B') \ln (1 + B')}\right]^{5/4} \qquad \text{(D-11)}$$

Equation (D-11) is useful for estimating the effect of blowing on boundary-layer closure in tubes.

SYMBOLS

a	speed of sound
B, B'	wall blowing parameters, Eqs. (D-2a) and (D-2b)
C_f, C_H	local shear and heat transfer coefficients, Eqs. (A-7a) and (A-7b)
h	static enthalpy per unit mass
h_r	recovery (adiabatic wall) value of h in laboratory coordinates, Eq. (A-2c)
M_s	shock Mach number, u_w/a_1
Pr	Prandtl number
p	pressure in atmospheres
$-q_w$	heat transfer to wall, $(k \partial T/\partial y)_w$
Re, $\bar{R}e$	Reynolds numbers
r(o)	recovery factor, $(Pr)^{1/3}$
T	temperature, degrees Rankine
u	velocity in x direction, shock-fixed coordinates
u_w	shock speed (wall velocity in shock-fixed coordinates)
u_e	free-stream velocity behind shock in shock-fixed coordinates
v_e	vertical velocity at edge of boundary layer
W	u_w/u_e, ρ_e/ρ_1
x	streamwise distance
γ	ratio specific heats
δ	boundary-layer thickness
δ^*	displacement thickness, shock-fixed coordinates

θ	momentum thickness, shock-fixed coordinates
μ	viscosity
υ	kinematic viscosity
ρ	density
τ_w	wall shear, $(\mu \partial u/\partial y)_w$

Subscripts

e	free stream downstream of shock
m	mean value
r	recovery value
w	wall value downstream of shock
0	zero wall blowing value
1	free-stream value upstream of shock

THE IVAN A. GETTING LABORATORIES

The Laboratory Operations of The Aerospace Corporation is conducting experimental and theoretical investigations necessary for the evaluation and application of scientific advances to new military concepts and systems. Versatility and flexibility have been developed to a high degree by the laboratory personnel in dealing with the many problems encountered in the nation's rapidly developing space and missile systems. Expertise in the latest scientific developments is vital to the accomplishment of tasks related to these problems. The laboratories that contribute to this research are:

Aerophysics Laboratory: Launch and reentry aerodynamics, heat transfer, reentry physics, chemical kinetics, structural mechanics, flight dynamics, atmospheric pollution, and high-power gas lasers.

Chemistry and Physics Laboratory: Atmospheric reactions and atmospheric optics, chemical reactions in polluted atmospheres, chemical reactions of excited species in rocket plumes, chemical thermodynamics, plasma and laser-induced reactions, laser chemistry, propulsion chemistry, space vacuum and radiation effects on materials, lubrication and surface phenomena, photosensitive materials and sensors, high precision laser ranging, and the application of physics and chemistry to problems of law enforcement and biomedicine.

Electronics Research Laboratory: Electromagnetic theory, devices, and propagation phenomena, including plasma electromagnetics; quantum electronics, lasers, and electro-optics; communication sciences, applied electronics, semiconducting, superconducting, and crystal device physics, optical and acoustical imaging; atmospheric pollution; millimeter wave and far-infrared technology.

Materials Sciences Laboratory: Development of new materials; metal matrix composites and new forms of carbon; test and evaluation of graphite and ceramics in reentry; spacecraft materials and electronic components in nuclear weapons environment; application of fracture mechanics to stress corrosion and fatigue-induced fractures in structural metals.

Space Sciences Laboratory: Atmospheric and ionospheric physics, radiation from the atmosphere, density and composition of the atmosphere, aurorae and airglow; magnetospheric physics, cosmic rays, generation and propagation of plasma waves in the magnetosphere; solar physics, studies of solar magnetic fields; space astronomy, x-ray astronomy; the effects of nuclear explosions, magnetic storms, and solar activity on the earth's atmosphere, ionosphere, and magnetosphere; the effects of optical, electromagnetic, and particulate radiations in space on space systems.

THE AEROSPACE CORPORATION
El Segundo, California